PHYSICAL REVIEW A VOLUME 37, NUMBER 9 MAY 1, 1988

Elastic scattering of ^{152}Eu and ^{154}Eu γ rays by atoms

J. P. Lestone, R. B. Taylor, P. Teansomprasong,* and I. B. Whittingham
Physics Department, James Cook University, Townsville, Australia 4811
(Received 9 November 1987)

Differential cross sections are reported for the elastic scattering of 344-, 411-, 444-, 723-, 779-, 868-, 964-, 1005-, 1086-, 1112-, 1275-, and 1408-keV γ rays through scattering angles from 2° to 45° by targets of Cu, Mo, Sn, Ta, Pb, and U. The results have been compared with two sets of theoretical cross sections for Rayleigh plus nuclear-Thomson plus Delbruck scattering. The first set was interpolated from the tables of P. P. Kane *et al.* [Phys. Rep. **140**, 75 (1986)], which are based upon exact S-matrix amplitudes for inner-shell Rayleigh scattering and use of modified form factors and photoelectric cross sections for outer-shell Rayleigh scattering; the second set was based upon modified-form-factor Rayleigh amplitudes for all electron shells. The measured cross sections agree to closer than 10% with the Kane *et al.* calculations and indicate that for larger scattering angles, higher photon energies, and heavier target elements the modified form factor overestimates Rayleigh scattering. At small scattering angles there is no evidence for any systematic discrepancy between experiment and the cross sections of Kane *et al.*

I. INTRODUCTION

The elastic scattering by atoms of γ rays of energies up to a few MeV has been the subject of intensive experimental investigation in an attempt to assess the accuracy of the theoretical cross sections computed from the contributing processes of Rayleigh, nuclear-Thomson, Delbruck, and nuclear-resonance scattering. A detailed investigation of the elastic scattering of ^{152}Eu and ^{154}Eu γ rays through small angles has already been published,[1] and the present work extends this investigation to larger angles where the differences between the various theoretical models are more marked.

For γ-ray energies below a few MeV the dominant process is Rayleigh scattering for which the most accurate calculations[2–4] are based upon the second-order S matrix in the bound-interaction picture, which allows for atomic binding effects on the initial, intermediate, and final electron states, and involves multipole expansions of the initial and final photon fields and numerical solution of inhomogeneous radial Dirac equations for each atomic subshell. These numerical partial-wave calculations require vast amounts of computer time and, consequently, have been restricted primarily to K- and L-shell scattering. For this reason the form-factor and modified-form-factor approximations of Franz[5] are still widely used to calculate Rayleigh scattering. In particular, modified form factors have recently been used by Kissel and Pratt[3,6] to obtain outer-shell Rayleigh scattering amplitudes which, when combined with the accurate inner-shell S-matrix calculations, yield total-atom Rayleigh amplitudes accurate to the order of 1%.

Of the remaining contributions to elastic scattering, nuclear-Thomson scattering is accurately described by the simple formula for classical scattering of an electromagnetic wave from a free structureless point charge (in this case the nucleus), Delbruck scattering has been calculated[7,8] to order $\alpha(\alpha Z)^2$ using the first Born approximation for the interaction of the virtual electron-positron pair with the nonquantized Coulomb field of the nucleus, and nuclear resonance scattering is negligible for the γ-ray energies considered in this investigation since the giant-dipole resonances are centered around $\approx 80\ A^{-1/3}$ MeV and have full widths at half maximum of a few MeV. These Delbruck and nuclear-Thomson amplitudes have been combined with the accurate Rayleigh amplitudes of Kissel and Pratt[3,6] to yield[4] theoretical elastic scattering cross sections with uncertainties conservatively estimated as 2%, thus surpassing the typical errors of 5–10% in the present experimental data. Kane *et al.*[4] also present a detailed comparison of existing experimental data with their theoretical cross sections and conclude that, although there is no evidence for any systematic disagreement between theory and experiment, the largest discrepancies do appear to occur at the smaller scattering angles and that, for the most extensive data set (Pb), the theoretical results lie below experiment for 145–412 keV and above experiment for 662–1332 keV.

Different ranges of scattering angle provide different checks on the adequacy of the theoretical calculations. For small-angle (that is, small-momentum-transfer) elastic scattering, Rayleigh scattering is the only significant contributing process to the cross section. Furthermore, in this region there will be major contributions to Rayleigh scattering from outer atomic subshells for which only form-factor amplitudes are available. Roy *et al.*[9] have shown that, for small momentum transfers, cross sections calculated with Rayleigh scattering represented by form-factor amplitudes (denoted NRFF) computed using nonrelativistic Hartree-Fock atomic wave functions, and modified form-factor amplitudes (denoted RMFF) computed using relativistic Dirac-Hartree-Fock-Slater (DHFS) atomic wave functions, agree closely with the S-matrix calculations of Kissel and Pratt,[3,6] whereas form-factor amplitudes (denoted RFF) computed using DHFS wave functions are too large.

At larger angles the differences between the various theoretical models for Rayleigh scattering are more marked, and the inclusion of Delbruck scattering is essential. Accurate measurements in this region can therefore test both the validity of the various treatments of Rayleigh scattering and of the Born-approximation Delbruck amplitudes.

A previous investigation[1] on small angle ($\theta \leq 10°$) scattering of Eu γ-rays yielded experimental data in good agreement with theoretical cross sections for Rayleigh plus nuclear-Thomson scattering based upon RMFF Rayleigh amplitudes. This present paper extends this investigation to larger scattering angles and reports on the scattering of 344-, 411-, 444-, 723-, 779-, 868-, 964-, 1005-, 1086-, 1112-, 1275-, and 1408-keV γ rays through scattering angles of 15°, 20°, 30°, and 45° by targets of Cu, Mo, Sn, Ta, Pb, and U. Low count rates restricted the Cu results to $\theta \leq 15°$, the Mo results to $\theta \leq 30°$, and the Sn results at 45° to energies below 779 keV. The use of a Eu γ-ray source allows simultaneous determination of cross sections for the different γ-ray energies, which reduces experimental running time and eliminates many sources of error, thus allowing all cross sections to be related back to one normalization point. The experimental cross sections are compared with theoretical cross sections for Rayleigh plus nuclear-Thomson plus Delbruck scattering interpolated from the tables of Kane *et al.*[4] Comparisons are also presented with the "best possible" form-factor model in which RMFF Rayleigh amplitudes are used. For completeness, tabulations of the present results also include the data for 2°, 3°, 5°, 7°, and 10° scattering which were discussed, but not tabulated, in our earlier investigation.[1] A preliminary report on some of the present results has already been published.[10]

II. THEORY

The differential cross section for elastic scattering of unpolarized γ rays of energy $\hbar\omega$ through an angle θ into the element of solid angle $d\Omega$ is

$$\frac{d\sigma}{d\Omega}=r_e^2\,|f(\omega,\theta)|^2\,, \tag{1}$$

where $f(\omega,\theta)$ is the total elastic scattering amplitude in units of the classical electron radius r_e. For γ-ray energies up to a few MeV, $f(\omega,\theta)$ is a coherent superposition of amplitudes for Rayleigh R, nuclear-Thompson T, Delbruck D, and nuclear resonance N scattering, i.e.,

$$f=R+T+D+N\ . \tag{2}$$

If each scattering process is described in terms of circularly polarized photons, then

$$\frac{d\sigma}{d\Omega}=r_e^2[\,|f^+(\omega,\theta)|^2+|f^-(\omega,\theta)|^2]\,, \tag{3}$$

where f^+ and f^- are the amplitudes for no-spin flip and spin flip, respectively, that is, for no change and change, respectively, in the state of circular polarization.

The exact calculations of Rayleigh scattering[2-4,6] are based upon the second-order S matrix for scattering of a photon of initial four-wave vector $k_i=(\omega,\mathbf{k}_i)$ and four-polarization $\epsilon^{(i)}=(0,\boldsymbol{\epsilon}^{(i)})$ into a state with $k_f=(\omega,\mathbf{k}_f)$ and $\epsilon^{(f)}=(0,\boldsymbol{\epsilon}^{(f)})$,

$$S=S^{(a)}+S^{(e)}\,, \tag{4}$$

where

$$S^{(a)}=\frac{r_e m_e c^2}{8\pi^2\hbar\omega}\int\int d^4x'd^4x\,\bar{\psi}(x')\gamma\epsilon^{(f)*}\times\exp(ik_fx')S^{(\mathrm{ext})}(x',x)\gamma\epsilon^{(i)}\times\exp(-ik_ix)\psi(x)\,, \tag{5}$$

and

$$S^{(e)}=S^{(a)}(k_f\leftrightarrow -k_i,\epsilon^{(f)*}\leftrightarrow\epsilon^{(i)})\ . \tag{6}$$

The γ^μ ($\mu=0,1,2,3$) are the Dirac matrices, $x^\mu=(ct,\mathbf{x})$, the atomic states $\psi(x)$ are solutions of the Dirac equation for an electron in an external field $A_\mu^{(\mathrm{ext})}$,

$$\left[i\gamma^\mu\frac{\partial}{\partial x^\mu}-\frac{e}{\hbar}\gamma^\mu A_\mu^{(\mathrm{ext})}(x)-\frac{m_ec}{\hbar}\right]\psi(x)=0\,, \tag{7}$$

and the bound-electron propagator $S^{(\mathrm{ext})}(x',x)$ satisfies

$$\left[i\gamma^\mu\frac{\partial}{\partial x^\mu}-\frac{e}{\hbar}\gamma^\mu A_\mu^{(\mathrm{ext})}(x)-\frac{m_ec}{\hbar}\right]S^{(\mathrm{ext})}(x',x)=-2i\delta^{(4)}(x-x')\ . \tag{8}$$

The calculational procedure developed by Brown and coworkers,[11] Johnson and coworkers,[2] and Kissel and Pratt[3,6] assumes a spherically symmetrical static external field $A_\mu^{(\mathrm{ext})}=(0,V(r)/c)$ and that the scattering is from an atom with filled subshells. The S matrix

$$S=r_eR_{jk}\epsilon_j^{(f)*}\epsilon_k^{(i)} \tag{9}$$

can then be written in terms of polarization vectors parallel $\epsilon_\parallel$ and perpendicular $\epsilon_\perp$ to the scattering plane as

$$S=r_eR^{\parallel}\epsilon_\parallel^{(f)*}\epsilon_\parallel^{(i)}+r_eR^{\perp}\epsilon_\perp^{(f)*}\epsilon_\perp^{(i)}\ . \tag{10}$$

In terms of circular polarization vectors

$$\epsilon_\pm=\mp\frac{1}{\sqrt{2}}(\epsilon_\parallel\pm i\epsilon_\perp)\,, \tag{11}$$

the amplitudes for no change R^+ and change R^-, respectively, in the state of circular polarization are

$$R^\pm=\tfrac{1}{2}(R^\perp\pm R^\parallel)\ . \tag{12}$$

A multipole expansion of the photon interaction terms

$$\mathbf{a}^{(i)}\equiv\epsilon^{(i)}\exp(-i\mathbf{k}_i\cdot\mathbf{x})$$

and $\mathbf{a}^{(f)*}$ then results in the Rayleigh amplitudes $R^{(\parallel,\perp)}$ being expressed as a sum over filled atomic subshells of multipole amplitudes constructed from the solutions of the inhomogeneous radial Dirac equations. Most of the calculations have used DHFS self-consistent potentials for $V(r)$ but have restricted the sum over subshells to the K-, L-, and, in some cases, M-shell electrons.

The widely used form-factor treatment of Rayleigh scattering[5,12] replaces the bound-electron propagator with the free-electron propagator, that is, atomic binding effects are neglected in the intermediate states, an approximation which requires the atomic binding energies $B_i = m_e c^2 - E_i$ to be much less than the photon energy $\hbar\omega$, and also that all momentum transfers to the atom to be much less than $m_e c$. The amplitudes for Rayleigh scattering from the ith atomic subshell are then

$$R_i^{\pm} = -\tfrac{1}{2}(1 \pm \cos\theta) f_i(q) \, , \tag{13}$$

where f_i is the atomic form factor

$$f_i(q) = \int d^3x \, \psi_i^\dagger(\mathbf{x}) \exp(i\mathbf{q}\cdot\mathbf{x}) \psi_i(\mathbf{x}) \tag{14}$$

and

$$\hbar q = (2\hbar\omega / c)\sin(\theta/2) \tag{15}$$

is the momentum transfer from the photon to the atom.

A detailed comparison of numerical S-matrix and form-factor predictions for Rayleigh scattering, both using DHFS atomic wave functions, shows[3] that, at high energies where the agreement is best, the form-factor amplitudes are satisfactory for $\hbar q \le 0.2 m_e c$, the error being about $0.5(\alpha Z/n)^2$, where n is the principal quantum number of the electron. For larger momentum transfers $\hbar q \gg 0.2 m_e c$ and high photon energies $\hbar\omega \gg B_i$, the DHFS form-factor predictions are too large, often by factors exceeding 2–10.

The modified form-factor treatment of Rayleigh scattering[5,13] replaces $f_i(q)$ by the modified atomic form factor

$$g_i(q) = \int d^3x \, \psi_i^\dagger(\mathbf{x}) \exp(i\mathbf{q}\cdot\mathbf{x}) \frac{m_e c^2}{E_i - V(r)} \psi_i(\mathbf{x}) \, , \tag{16}$$

where E_i is the energy of the atomic electron in state $\psi_i(\mathbf{x})$ and $V(r)$ is its potential energy. The additional factor $m_e c^2 (E_i - V)^{-1}$ in the g form factor represents a binding correction to the assumption of free intermediate-state electrons used in the f form factor. In fact, an expansion of the g form factor in powers of αZ yields the first- and second-order terms of the Born-approximation calculation of the S matrix performed by Brown and Woodward,[14] in which the bound intermediate states of the electron were expanded in terms of free states and potential scatterings. The factor $m_e c^2 (E_i - V)^{-1}$ tends to correct[3] the order $(\alpha Z)^2$ errors in the f form factor and, at high energies, the g form factor reproduces exactly the zero-angle Rayleigh amplitude at infinite photon energy calculated by Levinger and Rustgi.[15]

The modified form factor can be used for momentum transfers $\hbar q \le \hbar q_{\mathrm{typ}}$, where $\hbar q_{\mathrm{typ}} = \alpha Z m_e c / n^2$ is the typical momentum of electrons in the shell with principal quantum number n. Since the contribution to the Rayleigh amplitude of any shell is approximately constant and equal to the number of electrons in that shell, for $\hbar q \le \hbar q_{\mathrm{typ}}$, and then decreases monotonically until it is negligible at the typical momentum of the next innermost shell, the g form factor can generally be used for any shell other than the K shell. The K-shell scattering gives nearly the entire Rayleigh amplitude for $\hbar q \ge \alpha Z m_e c$.

As a consequence of the above observations, Pratt and co-workers[3,6] computed total-atom Rayleigh amplitudes according to the prescription of numerical S-matrix amplitudes R_j for the inner shells (usually K and L shells), and

$$\mathrm{Re} R_i^{\perp} = -g_i \, , \quad \mathrm{Re} R_i^{\parallel} = -g_i \cos\theta \, , \tag{17}$$

$$\mathrm{Im} R_i^{(\perp,\parallel)} = \frac{\sigma_i^{\mathrm{PE}}}{\sigma_j^{\mathrm{PE}}} \mathrm{Im} R_j^{(\perp,\parallel)} \, , \tag{18}$$

for the outer shells. σ_i^{PE} is the total photoelectric cross section for the ith shell and vanishes for $\hbar\omega < B_i$.

The amplitudes for nuclear-Thomson scattering from a nucleus of mass M and charge Ze are independent of photon energy and are given by

$$T^{\pm} = -\frac{Z^2 m_e}{2M}(1 \pm \cos\theta) \, , \tag{19}$$

and therefore have the same angular dependence as the form-factor Rayleigh amplitudes. The maximum (zero-angle) nuclear-Thomson contribution T^+ ranges from -0.0034 for Al to -0.0196 for U and is therefore relatively insignificant in comparison with the zero-angle Rayleigh amplitude $R^+(\omega,0) \approx -Z$. However, for momentum transfers $\hbar q \ge \hbar q_{\mathrm{typ}}$, where the form-factor Rayleigh amplitudes over estimate the Rayleigh amplitude, the nuclear-Thomson contribution increases in significance.

Delbruck scattering is the scattering of a photon by the static nonquantized Coulomb field of the nucleus. The incident photon creates an electron-positron pair, virtual or real depending on whether the photon energy is smaller or greater than $2m_e c^2$, which then interacts with the nuclear field before annihilating to produce the outgoing photon. The imaginary part of the Delbruck amplitude, corresponding to real pairs in the intermediate states, is closely related to the pair-production cross section and vanishes for photon energies below $2m_e c^2$. The real part of the amplitude corresponds to virtual pairs and is related to vacuum polarization.

The most accurate calculations of Delbruck scattering[7,8,16] use the first Born approximation for the intermediate-state pair to express the Delbruck amplitude in terms of the fourth-order vacuum polarization tensor. The electron and positron between interactions are then represented by the free-electron propagator and the Delbruck amplitude has the form $(\alpha Z)^2$ times a Z-independent amplitude. These Z-independent amplitudes have been computed[7,17] for a wide range of scattering angles and photon energies. These lowest-order Born predictions are expected to be accurate to a few percent for $Z < 60$, but for larger Z the higher-order Coulomb corrections of order $(\alpha Z)^{2n}$, $n = 2$, 3, or 4 can be significant (e.g., scattering of 2.75-MeV photons by Pu indicates that these terms modify the Delbruck amplitudes by more than 50%[18]).

For 1–4-MeV photons scattered by heavy atoms, strong interference occurs[3] between the contributions of Delbruck, nuclear-Thomson, and Rayleigh scattering, with Rayleigh and nuclear-Thomson amplitudes generally of the same sign, but with Delbruck scattering interfering destructively at smaller angles and constructively at larger angles. Nuclear-resonance scattering arises from excitation of the giant-dipole resonance which can be represented[19] by a Lorentzian, or superposition of two Lorentzians, centered around $\approx 80\ A^{-1/3}$ MeV and with width(s) of $\approx 3-5$ MeV. This nuclear-resonance scattering is negligible for γ-ray energies considered here and will be ignored.

Two sets of theoretical cross sections for Rayleigh plus nuclear-Thomson plus Delbruck scattering have been calculated for comparison with our experimental data. The first set, denoted $d\sigma^{\mathrm{KP}}$, were obtained by interpolation of the tables of Kane *et al.*[4] These cross sections use the above prescription of Kissel and Pratt[3] for the Rayleigh amplitudes, that is, numerical S-matrix amplitudes for inner-shell and Eqs. (17) and (18) for outer-shell amplitudes, and include nuclear-Thomson and Delbruck scattering calculated, respectively, from (19) and the program of Papatzacos and Mork.[7] The tables of cross sections were interpolated with respect to energy using both the method of cubic splines and the Fritsch and Carlson method[20] of monotonic piecewise cubic interpolation. The two methods give cross sections which agree to within a few percent. The second set of theoretical cross sections, denoted $d\sigma^{\mathrm{RMFF}}$, use RMFF Rayleigh amplitudes for all electrons, obtained from the computer program of Schaupp *et al.*[21] using input DHFS wave functions generated by the computer program of Liberman and Cromer.[22] The computed RMFF values agreed to better than 1% with values obtained by cubic-spline interpolation of the tabulations of Schaupp *et al.*[23] The lowest-order Born approximation Delbruck amplitudes used in $d\sigma^{\mathrm{RMFF}}$ were computed by Mork and Rotting[17] using the program of Papatzacos and Mork.[7] A comparison of the two sets of cross sections, together with cross sections calculated using nonrelativistic ($d\sigma^{\mathrm{NRFF}}$) and relativistic ($d\sigma^{\mathrm{RFF}}$) f form-factor Rayleigh amplitudes, indicates[24] that, whereas $d\sigma^{\mathrm{RMFF}}$ and $d\sigma^{\mathrm{KP}}$ agree closely for momentum transfers $x \equiv \lambda^{-1}\sin(\theta/2)$ as large as 40 Å^{-1}, $d\sigma^{\mathrm{RFF}}$ and $d\sigma^{\mathrm{NRFF}}$ become far too large for $x \geq 10$ Å^{-1}, the discrepancy increasing rapidly with x, $\hbar\omega$, and Z.

III. EXPERIMENTAL DETAILS AND RESULTS

The experimental details differ from those of our previous investigation[1] only in that a stronger γ-ray source was used. The γ rays from a 3-Ci source containing ^{152}Eu and ^{154}Eu were scattered into a Ge(Li) detector which had a resolution of 2.5 keV full width at half maximum (FWHM) at 1330 keV. At each scattering angle, experimental runs were done with thick and thin targets of each element studied in order to check for multiple-scattering effects, with a carbon target to obtain a Compton line shape, and with a 0.1-mCi source containing ^{152}Eu and ^{154}Eu placed at the target position to obtain the elastic line shape. These runs were interspersed with no-target runs to obtain background spectra. All spectra were recorded by a 4096-channel pulse-height analyzer.

If $I(\omega,Z,\theta,t)$ is the intensity in the elastic or Compton peak for scattering of a photon of incident energy $\hbar\omega$ through an angle θ from a target of atomic number Z and thickness t, the associated differential cross section is given by

$$\frac{d\sigma(\omega,Z,\theta)}{d\Omega} = \frac{I(\omega,Z,\theta,t)}{G_{\mathrm{ST}}G_{\mathrm{TD}}N(\omega)\epsilon(\omega')n_Z T(\omega,Z,\theta,t)}\ , \tag{20}$$

where G_{ST} and G_{TD} are source-target and target-detector geometrical factors, $N(\omega)$ is the source strength of γ rays of energy $\hbar\omega$ after correction for radioactive decay, $\epsilon(\omega')$ is the detector photopeak efficiency at the scattered photon energy $\hbar\omega'$, n_Z is the atomic density of the target, and

$$T = \int_0^t e^{-\mu x} e^{-\mu' x (t-x)\sec\theta} dx \tag{21}$$

is the target transmission factor where μ and μ' are the target linear-attenuation coefficients for the incident and scattered photon energies, respectively. The thin target thicknesses were chosen so that $\mu t = 1$ for 344 keV γ rays, the thick targets such that $\mu t = 1$ for 779 keV.

Ratios of elastic scattering cross sections at different angles, and of elastic to Compton scattering cross sections at a given angle, were directly obtained[1] from the intensities of the elastic and Compton peaks in the scattered photon spectrum. Absolute elastic cross sections were obtained by normalizing to the theoretical carbon Compton cross section at 7° taken to be the Klein-Nishina cross section multiplied by the incoherent scattering function. The cross sections change by less than 10% if the normalization is changed to the theoretical carbon Compton cross section at 3°, 5°, or 10° or if theoretical aluminum Compton cross sections at 3°, 5°, or 7° are used.

For those angles and energies where the elastic and Compton peaks overlap, their relative intensities were extracted using a least-squares method based upon the experimentally measured elastic and carbon Compton line shapes. Previous analyses[1,25,26] had assumed that the Compton line shapes were independent of the target material but recently Dow *et al.*[27] have established that the widths of the Compton peaks increase slightly with increasing atomic number and photon energy. To allow for this effect, the elastic and Compton intensities of a target spectrum were extracted using a least-squares method based upon the Compton line shapes of the carbon spectrum and the elastic line shapes of the Eu spectrum, where the carbon Compton profiles were broadened for each element by convoluting the carbon Compton profile with a Gaussian of FWHM w_B and varying w_B until a best fit was obtained. This effect is significant in the determination of elastic cross sections only where the elastic peak is very small compared to the overlapping Compton peak. Only the results at 5° and 7° needed to be corrected for this Z dependence of the Compton line shapes, and at these angles the correction was significant only for Cu and Mo for γ-ray energies ≥ 964 keV and for Sn and Ta for energies ≥ 1.005 MeV. The correction was less than 5% for the Pb and U targets. The maximum correction was about 38% for the case of 1408-keV γ rays scattered from the Cu target at 5°. The experimental results, together with the theoretical cross sections ($d\sigma^{\mathrm{KP}}$ for γ-ray energies from 344–1275 keV and $d\sigma^{\mathrm{RMFF}}$ for 1408 keV γ rays), are given in Tables I–VI. Compar-

TABLE I. Experimental and theoretical differential cross sections for the elastic scattering of Eu γ rays by Cu (b/sr). Exponents are given in square brackets.

Energy (keV)	Scattering angle (deg) 2	3	5	7	10	15	20	30	45
344									
Expt.	1.21±0.16[1]	9.22±0.93[0]	2.79±0.28[0]	1.38±0.15[0]	7.70±1.00[−1]	1.46±0.20[−1]			
KP	1.61[1]	7.20[0]	2.87[0]	1.65[0]	6.50[−1]	1.75[−1]	8.54[−2]	3.34[−2]	6.99[−3]
411									
Expt.	1.10±0.14[1]	5.41±0.54[0]	2.37±0.24[0]	1.02±0.13[0]	4.57±0.64[−1]	8.80±1.30[−2]			
KP	1.15[1]	5.00[0]	2.23[0]	1.12[0]	3.47[−1]	1.09[−1]	6.29[−2]	1.90[−2]	2.73[−3]
444									
Expt.	1.05±0.14[1]	4.73±0.47[0]	1.77±0.23[0]	6.73±0.87[−1]	2.94±0.41[−1]	6.60±1.00[−2]			
KP	9.92[0]	4.36[0]	1.95[0]	9.09[−1]	2.71[−1]	9.17[−2]	5.33[−2]	1.42[−2]	1.77[−3]
723									
Expt.	3.30±0.73[0]	1.79±0.23[0]	5.00±2.10[−1]	1.78±0.38[−1]	9.90±2.10[−2]				
KP	3.78[0]	2.03[0]	5.48[−1]	1.80[−1]	8.14[−2]	3.18[−2]	1.04[−2]	1.17[−3]	8.46[−5]
779									
Expt.	3.16±0.35[0]	1.83±0.18[0]	4.11±0.53[−1]	1.65±0.21[−1]	5.70±0.80[−2]	2.20±0.30[−2]			
KP	3.36[0]	1.78[0]	4.20[−1]	1.47[−1]	7.11[−2]	2.47[−2]	7.35[−3]	7.34[−4]	5.14[−5]
868									
Expt.	2.83±0.51[0]	1.28±0.20[0]	2.71±0.92[−1]	1.51±0.27[−1]	6.00±1.20[−2]	1.47±0.37[−2]			
KP	2.85[0]	1.43[0]	2.87[−1]	1.14[−1]	5.77[−2]	1.62[−2]	4.30[−3]	3.66[−4]	2.54[−5]
964									
Expt.	2.28±0.23[0]	1.20±0.16[0]	2.24±0.48[−1]	1.03±0.12[−1]	4.40±0.60[−2]	8.80±1.30[−3]			
KP	2.52[0]	1.08[0]	2.10[−1]	9.66[−2]	4.71[−2]	1.06[−2]	2.39[−3]	1.83[−4]	1.35[−5]
1005									
Expt.	2.49±0.57[0]	8.20±1.80[−1]	2.39±0.98[−1]	1.11±0.29[−1]	5.30±1.50[−2]				
KP	2.35[0]	9.68[−1]	1.86[−1]	8.86[−2]	4.21[−2]	8.71[−3]	1.87[−3]	1.37[−4]	1.07[−5]
1086									
Expt.	1.49±0.21[0]	7.70±0.80[−1]	1.70±0.37[−1]	7.50±1.60[−2]	3.80±0.70[−2]	4.75±0.95[−3]			
KP	2.04[0]	7.71[−1]	1.52[−1]	7.54[−2]	3.31[−2]	5.92[−3]	1.16[−3]	7.97[−5]	6.99[−6]
1112									
Expt.	1.36±0.18[0]	7.13±0.78[−1]	1.70±0.37[−1]	7.50±1.60[−2]	3.26±0.42[−2]	4.46±0.80[−3]			
KP	1.95[0]	7.16[−1]	1.44[−1]	7.18[−2]	3.05[−2]	5.23[−3]	1.00[−3]	6.72[−5]	6.17[−6]
1275									
Expt.	1.01±0.26[0]	3.58±0.77[−1]	1.15±0.59[−1]	5.60±1.10[−2]	1.32±0.45[−2]				
KP	1.47[0]	4.45[−1]	1.06[−1]	5.36[−2]	1.77[−2]	2.41[−3]	3.96[−4]	2.40[−5]	3.06[−6]
1408									
Expt.	9.20±1.70[−1]	2.44±0.39[−1]	7.80±1.70[−2]	4.30±0.50[−2]	1.25±0.16[−2]	1.13±0.19[−3]			
RMFF	1.17[0]	3.10[−1]	8.97[−2]	4.29[−2]	1.18[−2]	1.35[−3]	2.02[−4]	1.19[−5]	2.09[−6]

TABLE II. Experimental and theoretical differential cross sections for the elastic scattering of Eu γ rays by Mo (b/sr). Exponents are given in square brackets.

Energy (keV)	Scattering angle (deg) 2	3	5	7	10	15	20	30	45
344									
Expt.	3.94±0.51[1]	2.10±0.23[1]	8.29±0.83[0]	3.54±0.39[0]	2.16±0.26[0]	5.98±0.72[−1]	2.60±0.28[−1]	7.06±0.92[−2]	
KP	3.90[1]	2.31[1]	8.24[0]	3.67[0]	1.78[0]	6.57[−1]	2.53[−1]	7.83[−2]	2.70[−2]
411									
Expt.	3.49±0.38[1]	1.70±0.20[1]	5.29±0.58[0]	2.49±0.32[0]	1.59±0.19[0]	2.66±0.32[−1]	1.32±0.14[−1]	5.10±1.10[−2]	
KP	3.16[1]	1.73[1]	5.16[0]	2.50[0]	1.29[0]	3.55[−1]	1.38[−1]	5.51[−2]	1.53[−2]
444									
Expt.	2.68±0.29[1]	1.33±0.17[1]	4.14±0.45[0]	2.06±0.25[0]	1.14±0.14[0]	2.11±0.27[−1]	1.10±0.14[−1]	4.80±0.77[−2]	
KP	2.86[1]	1.49[1]	4.32[0]	2.14[0]	1.07[0]	2.76[−1]	1.12[−1]	4.60[−2]	1.14[−2]
723									
Expt.	1.07±0.16[1]	4.04±0.53[0]	1.65±0.25[0]	6.56±0.98[−1]	2.25±0.34[−1]		3.60±0.25[−2]	8.50±2.10[−3]	
KP	1.26[1]	4.56[0]	1.67[0]	7.18[−1]	2.07[−1]	7.51[−2]	3.94[−2]	8.46[−3]	8.60[−4]
779									
Expt.	100±0.10[1]	3.59±0.39[0]	1.41±0.15[0]	6.16±0.68[−1]	1.67±0.20[−1]	5.68±0.80[−2]	3.00±0.50[−2]	6.70±1.10[−3]	
KP	1.05[1]	3.82[0]	1.43[0]	5.54[−1]	1.65[−1]	6.48[−2]	3.18[−2]	5.88[−3]	5.30[−4]
868									
Expt.	8.90±0.85[0]	3.30±0.32[0]	1.09±0.15[0]	3.81±0.53[−1]	1.50±0.24[−1]	4.36±0.87[−2]	2.10±0.35[−2]		
KP	7.99[0]	3.01[0]	1.12[0]	3.74[−1]	1.22[−1]	5.18[−2]	2.20[−2]	3.31[−3]	2.56[−4]
964									
Expt.	6.97±0.69[0]	2.22±0.20[0]	8.40±0.90[−1]	2.83±0.28[−1]	9.30±1.10[−2]	2.96±0.47[−2]	1.50±0.10[−2]	1.96±0.43[−3]	
KP	6.18[0]	2.44[0]	.8.41[−1]	2.63[−1]	9.46[−2]	3.95[−2]	1.45[−2]	1.80[−3]	1.23[−4]
1005									
Expt.	5.73±0.86[0]	2.07±0.25[0]	9.90±1.90[−1]	2.78±0.50[−1]	1.05±0.26[−1]		1.11±0.22[−2]		
KP	5.59[0]	2.25[0]	7.43[−1]	2.30[−1]	8.57[−2]	3.50[⊦2]	1.21[−2]	1.39[−3]	9.16[−5]
1086									
expt.	5.40±0.51[0]	2.06±0.19[0]	5.59±0.61[−1]	1.75±0.19[−1]	9.30±2.10[−2]	2.21±0.38[−2]	9.50±0.80[−3]	1.01±0.27[−3]	
KP	4.63[0]	1.93[0]	5.80[−1]	1.80[−1]	7.17[−2]	2.73[−2]	8.50[−3]	8.38[−4]	5.19[−5]
1112									
Expt.	4.69±0.45[0]	1.82±0.16[0]	5.59±0.61[−1]	1.75±0.19[−1]	7.10±0.90[−2]	2.18±0.39[−2]	7.60±0.50[−3]	9.30±2.00[−4]	
KP	4.37[0]	1.85[0]	5.35[−1]	1.67[−1]	6.81[−2]	2.52[−2]	7.57[−3]	7.13[−4]	4.34[−5]
1275									
Expt.	3.35±0.44[0]	1.03±0.18[0]	2.94±0.91[−1]	1.28±0.22[−1]	4.30±1.10[−2]	1.55±0.50[−2]	4.00±1.00[−3]		
KP	3.16[0]	1.45[0]	3.19[−1]	1.14[−1]	5.19[−2]	1.48[−2]	3.62[−3]	2.62[−4]	1.51[−5]
1408									
Expt.	2.85±0.31[0]	9.00±1.00[−1]	2.43±0.36[−1]	9.10±0.90[−2]	4.00±0.40[−2]	1.04±0.12[−2]	2.60±0.30[−3]	1.54±0.57[−4]	
RMFF	2.58[0]	1.19[0]	2.21[−1]	9.12[−2]	4.23[−2]	9.69[−3]	2.08[−3]	1.33[−4]	8.51[−6]

TABLE III. Experimental and theoretical differential cross sections for the elastic scattering of Eu γ rays by Sn (b/sr). Exponents are given in square brackets.

Energy (keV)	Scattering angle (deg) 2	3	5	7	10	15	20	30	45
344									
Expt.	4.21±0.55[1]	2.71±0.30[1]	1.49±0.15[1]	5.59±0.61[0]	2.63±0.20[0]	1.07±0.13[0]	4.75±0.20[−1]	1.18±0.15[−1]	4.04±0.46[−2]
KP	5.55[1]	3.23[1]	1.46[1]	6.55[0]	2.67[0]	1.08[0]	4.76[−1]	1.24[−1]	4.04[−2]
4.11									
Expt.	4.45±0.49[1]	2.34±0.28[1]	9.90±1.10[0]	4.41±0.57[0]	1.71±0.16[0]	6.26±0.75[−1]	2.40±0.18[−1]	7.00±1.50[−2]	2.15±0.23[−2]
KP	4.37[1]	2.53[1]	9.99[0]	3.94[0]	1.83[0]	6.99[−1]	2.50[−1]	7.61[−2]	2.68[−2]
444									
Expt.	3.32±0.37[1]	1.85±0.24[1]	7.80±0.80[0]	3.56±0.43[0]	1.52±0.16[0]	4.54±0.59[−1]	2.00±0.16[−1]	7.00±1.10[−2]	2.70±0.32[−2]
KP	3.95[1]	2.25[1]	8.29[0]	3.26[0]	1.54[0]	5.57[−1]	1.95[−1]	6.26[−2]	2.13[−2]
723									
Expt.	1.72±0.26[1]	6.44±0.84[0]	2.19±0.33[0]	9.90±1.50[−1]	4.10±0.40[−1]		5.26±0.50[−2]	1.67±0.42[−2]	
KP	2.00[1]	8.64[0]	2.31[0]	1.19[0]	4.10[−1]	1.07[−1]	5.65[−2]	1.73[−2]	2.30[−3]
779									
Expt.	1.50±0.15[1]	6.17±0.68[0]	1.98±0.22[0]	1.07±0.12[0]	3.20±0.15[−1]	8.80±1.20[−2]	4.45±0.32[−2]	1.29±0.21[−2]	
KP	1.77[1]	7.00[0]	2.01[0]	9.88[−1]	3.09[−1]	9.02[−2]	4.78[−2]	1.28[−2]	1.48[−3]
868									
Expt.	1.8±0.11[1]	5.14±0.51[0]	1.55±0.22[0]	7.40±1.00[−1]	2.39±0.20[−1]	7.80±1.60[−2]	3.48±0.50[−2]		
KP	1.46[1]	5.14[0]	1.66[0]	7.30[−1]	2.07[−1]	7.20[−2]	3.67[−2]	7.78[−3]	7.46[−4]
964									
Expt.	1.04±0.09[1]	3.58±0.32[0]	1.34±0.15[0]	5.54±0.55[−1]	1.50±0.11[−1]	5.90±0.90[−2]	2.66±0.19[−2]	4.60±1.00[−3]	
KP	1.17[1]	3.91[0]	1.33[0]	5.27[−1]	1.48[−1]	5.68[−2]	2.67[−2]	4.53[−3]	3.68[−4]
1005									
Expt.	1.00±0.15[1]	3.43±0.41[0]	1.29±0.25[0]	5.02±0.9[−1]	1.38±0.19[−1]		2.21±0.26[−2]		
KP	1.06[1]	3.53[0]	1.20[0]	4.60[−1]	1.31[−1]	5.13[−2]	2.31[−2]	3.60[−3]	2.74[−4]
1086									
Expt.	7.88±0.75[0]	3.01±0.27[0]	9.30±1.00[−1]	3.61±0.40[−1]	1.01±0.11[−1]	3.60±0.60[−2]	1.71±0.13[−2]	2.65±0.72[−3]	
KP	8.77[0]	2.92[0]	9.88[−1]	3.52[−1]	1.05[−1]	4.20[−2]	1.73[−2]	2.28[−3]	1.54[−4]
1112									
Expt.	7.65±0.74[0]	2.77±0.25[0]	9.30±1.00[−1]	3.61±0.40[−1]	9.40±0.50[−2]	3.77±0.68[−2]	1.62±0.09[−2]	2.13±0.47[−3]	
KP	8.24[0]	2.76[0]	9.26[−1]	3.24[−1]	9.86[−2]	3.94[−2]	1.57[−2]	1.97[−3]	1.29[−4]
1275									
Expt.	5.28±0.69[0]	1.64±0.28[0]	5.20±1.60[−1]	2.21±0.38[−1]	7.10±0.40[−2]	2.61±0.81[−2]	1.03±0.11[−2]	1.09±0.44[−3]	
KP	5.52[0]	2.06[0]	6.13[−1]	1.92[−1]	7.25[−2]	2.65[−2]	8.44[−3]	7.85[−4]	4.24[−5]
1408									
Expt.	4.57±0.50[0]	1.41±0.16[0]	4.60±0.70[−1]	1.52±0.15[−1]	5.40±0.60[−2]	1.98±0.24[−2]	6.00±0.50[−3]	4.60±1.70[−4]	
RMFF	4.12[0]	1.72[0]	4.38[−1]	1.36[−1]	6.07[−2]	1.95[[illegible]]	5.34[−3]	4.32[−4]	2.33[−5]

TABLE IV. Experimental and theoretical differential cross sections for the elastic scattering of Eu γ rays by Ta (b/sr). Exponents are given in square brackets.

Energy (keV)	Scattering angle (deg) 2	3	5	7	10	15	20	30	45
344									
Expt.	1.23±0.16[2]	7.86±0.79[1]	3.46±0.35[1]	1.61±0.16[1]	1.02±0.11[1]	2.98±0.36[0]	1.37±0.19[0]	4.83±0.63[−1]	1.08±0.14[−1]
KP	1.48[2]	8.39[1]	3.30[1]	1.81[1]	8.78[0]	2.99[0]	1.43[0]	4.70[−1]	1.10[−1]
411									
Expt.	1.23±0.16[2]	6.25±0.64[1]	2.49±0.25[1]	1.27±0.13[1]	7.11±0.85[0]	1.98±0.26[0]	6.24±0.87[−1]	2.10±0.46[−1]	4.80±1.10[−2]
KP	1.18[2]	6.22[1]	2.36[1]	1.34[1]	5.61[0]	1.79[0]	9.81[−1]	2.55[−1]	6.03[−2]
444									
Expt.	9.20±1.10[1]	4.52±0.52[1]	1.85±0.18[1]	1.08±0.12[1]	4.38±0.53[0]	1.41±0.18[0]	5.32±0.72[−1]	2.05±0.29[−1]	4.75±0.76[−2]
KP	1.06[2]	5.42[1]	2.06[1]	1.14[1]	4.57[0]	1.47[0]	8.01[−1]	1.98[−1]	4.81[−2]
723									
Expt.	4.07±0.53[1]	1.93±0.25[1]	7.45±0.89[0]	2.95±0.35[0]	1.36±0.18[0]	4.26±0.89[−1]	1.90±0.42[−1]	4.68±0.75[−2]	
KP	4.60[1]	2.13[1]	8.00[0]	3.00[0]	1.26[0]	4.33[−1]	1.44[−1]	4.40[−2]	1.29[−2]
779									
Expt.	3.92±0.39[1]	1.94±0.19[1]	6.40±0.64[0]	2.65±0.26[0]	1.04±0.11[0]	3.29±0.46[−1]	9.90±1.40[−2]	3.79±0.49[−2]	9.60±2.10[−3]
KP	3.96[1]	1.89[1]	6.46[0]	2.44[0]	1.08[0]	3.24[−1]	1.12[−1]	3.69[−2]	9.53[−3]
868									
Expt.	3.33±0.37[1]	1.47±0.15[1]	4.47±0.45[0]	1.98±0.20[0]	8.70±1.00[−1]	2.24±0.45[−1]	8.40±1.50[−2]		
KP	3.19[1]	1.58[1]	4.66[0]	1.84[0]	8.54[−1]	2.09[−1]	7.98[−2]	2.82[−2]	5.78[−3]
964									
Expt.	2.83±0.25[1]	1.21±0.11[1]	3.45±0.31[0]	1.52±0.15[0]	6.40±0.60[−1]	1.37±0.19[−1]	6.00±0.80[−2]	2.03±0.30[−2]	3.36±0.47[−3]
KP	2.62[1]	1.29[1]	3.46[0]	1.43[0]	6.45[−1]	1.43[−1]	5.93[−2]	2.05[−2]	3.34[−3]
1005									
Expt.	2.31±0.28[1]	1.06±0.12[1]	2.39±0.37[0]	1.36±0.15[0]	6.40±1.20[−1]	1.36±0.35[−1]			
KP	2.43[1]	1.19[1]	3.08[0]	1.29[0]	5.68[−1]	1.24[−1]	5.28[−2]	1.77[−2]	2.64[−3]
1086									
Expt.	2.30±0.20[1]	9.40±0.90[0]	2.60±0.23[0]	1.17±0.12[0]	5.50±0.80[−1]	9.40±1.30[−2]	4.10±0.60[−2]	1.42±0.20[−2]	1.67±0.33[−3]
KP	2.11[1]	1.00[1]	2.49[0]	1.07[0]	4.37[−1]	9.56[−2]	4.28[−2]	1.31[−2]	1.66[−3]
1112									
Expt.	2.03±0.18[1]	8.40±0.80[0]	2.60±0.23[0]	1.17±0.12[0]	4.50±0.40[−1]	9.60±1.20[−2]	3.60±0.50[−2]	1.05±0.17[−2]	1.43±0.27[−3]
KP	2.03[1]	9.47[0]	2.34[0]	1.01[0]	4.01[−1]	8.88[−2]	4.02[−2]	1.19[−2]	1.43[−3]
1275									
Expt.	1.64±0.16[1]	5.80±0.60[0]	1.63±0.21[0]	7.30±1.00[−1]	2.26±0.67[−1]	5.60±0.80[−2]		7.30±1.20[−3]	6.70±1.80[−4]
KP	1.61[1]	6.71[0]	1.65[0]	7.50[−1]	2.28[−1]	6.04[−2]	2.88[−2]	6.22[−3]	5.61[−4]
1408									
Expt.	1.36±0.12[1]	5.00±0.50[0]	1.27±0.14[0]	6.15±0.61[−1]	2.05±0.20[−1]	5.10±0.60[−2]	2.05±0.30[−2]	4.50±0.60[−3]	2.90±0.90[−4]
RMFF	1.36[1]	5.03[0]	1.33[0]	5.81[−1]	1.53[−1]	5.02[−2]	2.39[−2]	4.34[−3]	3.52[−4]

TABLE V. Experimental and theoretical differential cross sections for the elastic scattering of Eu γ rays by Pb (b/sr). Exponents are given in square brackets.

Energy (keV)	Scattering angle (deg) 2	3	5	7	10	15	20	30	45
344									
Expt.	1.33±0.17[2]	1.02±0.10[2]	5.09±0.51[1]	2.37±0.24[1]	1.22±0.05[1]	4.62±0.55[0]	2.00±0.15[0]	7.00±0.90[−1]	1.66±0.07[−1]
KP	1.91[2]	1.15[2]	4.69[1]	2.36[1]	1.18[1]	4.37[0]	1.99[0]	6.83[−1]	1.72[−1]
411									
Expt.	1.46±0.19[2]	8.10±0.90[1]	3.38±0.34[1]	1.64±0.18[1]	8.30±0.30[0]	2.86±0.37[0]	1.13±0.09[0]	3.56±0.78[−1]	6.90±1.00[−2]
KP	1.56[2]	8.81[1]	3.22[1]	1.66[1]	8.33[0]	2.49[0]	1.26[0]	4.18[−1]	8.44[−2]
444									
Expt.	1.12±0.13[2]	5.72±0.69[1]	2.50±0.25[1]	1.38±0.15[1]	6.80±0.30[0]	1.96±0.25[0]	1.02±0.07[0]	3.26±0.46[−1]	7.10±0.60[−2]
KP	1.41[2]	7.73[1]	2.76[1]	1.42[1]	6.90[0]	2.02[0]	1.03[0]	3.26[−1]	6.54[−2]
723									
Expt.	4.91±0.64[1]	2.57±0.33[1]	1.08±0.13[1]	4.36±0.52[0]	1.70±0.10[0]	5.60±1.20[−1]	2.45±0.15[−1]	6.40±1.00[−2]	1.78±0.37[−2]
KP	6.62[1]	2.86[1]	1.08[1]	4.64[0]	1.64[0]	6.54[−1]	2.38[−1]	5.58[−2]	1.80[−2]
779									
Expt.	4.92±0.49[1]	2.29±0.23[1]	9.30±0.90[0]	3.94±0.39[0]	1.42±0.05[0]	5.14±0.72[−1]	1.82±0.25[−1]	4.80±0.60[−2]	1.32±0.29[−2]
KP	5.71[1]	2.44[1]	9.19[0]	3.64[0]	1.40[0]	5.12[−1]	1.76[−1]	4.63[−2]	1.41[−2]
868									
Expt.	3.95±0.43[1]	1.90±0.19[1]	6.70±0.70[0]	2.79±0.28[0]	1.25±0.10[0]	3.50±0.70[−1]	1.15±0.09[−1]		
KP	4.57[1]	1.96[1]	7.12[0]	2.56[0]	1.13[0]	3.48[−1]	1.15[−1]	3.59[−2]	9.33[−3]
964									
Expt.	3.74±0.34[1]	1.64±0.15[1]	5.50±0.50[0]	2.17±0.22[0]	9.06±0.29[−1]	2.45±0.34[−1]	8.40±1.00[−2]	2.71±0.41[−2]	5.90±0.20[−3]
KP	3.68[1]	1.60[1]	5.41[0]	1.91[0]	8.80[−1]	2.37[−1]	7.97[−2]	2.70[−2]	5.84[−3]
1005									
Expt.	3.42±0.41[1]	1.48±0.16[1]	5.40±0.60[0]	1.80±0.20[0]	8.60±0.80[−1]	2.42±0.63[−1]	6.62±0.72[−2]		4.40±1.00[−3]
KP	3.38[1]	1.47[1]	4.81[0]	1.71[0]	7.88[−1]	2.04[−1]	6.95[−2]	2.38[−2]	4.77[−3]
1086									
Expt.	2.96±0.27[1]	1.25±0.12[1]	3.94±0.35[0]	1.49±0.15[0]	6.60±0.60[−1]	1.46±0.20[−1]	5.60±0.30[−2]	1.79±0.35[−2]	3.20±0.40[−3]
KP	2.87[1]	1.27[1]	3.83[0]	1.41[0]	6.30[−1]	1.52[−1]	5.48[−2]	1.84[−2]	3.17[−3]
1112									
Expt.	2.66±0.24[1]	1.20±0.12[1]	3.94±0.35[0]	1.49±0.15[0]	6.10±0.26[−1]	1.46±0.18[−1]	5.30±0.20[−2]	1.43±0.23[−2]	2.80±0.10[−3]
KP	2.73[1]	1.21[1]	3.56[0]	1.34[0]	5.85[−1]	1.39[−1]	5.12[−2]	1.69[−2]	2.78[−3]
1275									
Expt.	1.89±0.19[1]	7.80±0.90[0]	2.23±0.29[0]	1.08±0.15[0]	3.70±0.20[−1]	9.40±1.40[−2]	4.00±0.40[−2]	1.01±0.16[−2]	1.56±0.30[−3]
KP	2.04[1]	9.39[0]	2.27[0]	1.02[0]	3.66[−1]	8.27[−2]	3.65[−2]	9.95[−3]	1.19[−3]
1408									
Expt.	1.79±0.16[1]	6.80±1.60[0]	1.80±0.20[0]	8.00±0.80[−1]	2.50±0.14[−1]	7.10±0.90[−2]	2.75±0.30[−2]	7.50±0.50[−3]	7.30±2.00[−4]
RMFF	1.68[1]	7.58[0]	1.70[0]	8.34[−1]	2.53[−1]	6.34[−2]	3.19[−2]	7.72[−3]	8.19[−4]

TABLE VI. Experimental and theoretical differential cross sections for the elastic scattering of Eu γ rays by U (b/sr). Exponents are given in square brackets.

Energy (keV)	Scattering angle (deg) 2	3	5	7	10	15	20	30	45
344									
Expt.	1.57±0.20[2]	1.41±0.14[2]	6.04±0.60[1]	2.78±0.28[1]	1.60±0.32[1]	6.93±0.83[0]	2.60±0.36[0]	1.00±0.13[0]	3.15±0.59[−1]
KP	2.42[2]	1.51[2]	6.65[1]	3.27[1]	1.55[1]	6.27[0]	2.84[0]	9.56[−1]	2.72[−1]
411									
Expt.	2.03±0.26[2]	1.35±0.15[2]	5.75±0.57[1]	2.16±0.24[1]	1.12±0.16[1]	4.52±0.59[0]	1.32±0.18[0]	5.80±1.30[−1]	1.01±0.19[−1]
KP	1.99[2]	1.16[2]	4.63[1]	2.16[1]	1.11[1]	3.88[0]	1.61[0]	6.43[−1]	1.35[−1]
444									
Expt.	1.83±0.22[2]	8.97±1.14[1]	4.43±0.44[1]	1.79±0.20[1]	9.70±1.40[0]	3.26±0.42[0]	1.04±0.15[0]	5.50±0.80[−1]	1.09±0.15[−1]
KP	1.81[2]	1.03[2]	3.93[1]	1.84[1]	9.30[0]	3.15[0]	1.31[0]	5.14[−1]	1.02[−1]
723									
Expt.	8.90±1.20[1]	3.48±0.45[1]	1.31±0.16[1]	5.00±0.60[0]	2.89±0.28[0]	7.30±1.50[−1]	3.83±0.84[−1]	8.10±1.30[−2]	2.22±0.47[−2]
KP	9.10[1]	4.14[1]	1.36[1]	6.85[0]	2.37[0]	8.77[−1]	3.96[−1]	7.99[−2]	2.33[−2]
779									
Expt.	7.49±0.75[1]	3.43±0.34[1]	1.16±0.12[1]	5.59±0.56[0]	2.06±0.27[0]	7.30±1.00[−1]	2.15±0.30[−1]	6.20±0.80[−2]	1.51±0.21[−2]
KP	7.99[1]	3.47[1]	1.19[1]	5.53[0]	1.93[0]	7.32[−1]	2.96[−1]	6.29[−2]	1.89[−2]
868									
Expt.	6.73±0.74[1]	2.71±0.27[1]	8.80±0.90[0]	3.61±0.36[0]	1.60±0.30[0]	4.90±1.00[−1]	1.80±0.32[−1]		
KP	6.55[1]	2.69[1]	9.78[0]	3.97[0]	1.45[0]	5.54[−1]	1.88[−1]	4.57[−2]	1.37[−2]
964									
Expt.	5.55±0.50[1]	2.19±0.20[1]	7.23±1.65[0]	2.60±0.26[0]	1.11±0.09[0]	3.88±0.54[−1]	1.21±0.17[−1]	3.50±0.50[−2]	9.48±0.53[−3]
KP	5.32[1]	2.14[1]	7.76[0]	2.92[0]	1.11[0]	4.01[−1]	1.25[−1]	3.37[−2]	9.32[−3]
1005									
Expt.	5.01±0.65[1]	1.63±0.24[1]	7.00±1.00[0]	2.37±0.36[0]	1.05±0.15[0]				
KP	4.87[1]	1.95[1]	7.00[0]	2.59[0]	9.97[−1]	3.47[−1]	1.07[−1]	2.97[−2]	7.87[−3]
1086									
Expt.	4.52±0.41[1]	1.73±0.17[1]	5.24±0.47[0]	1.85±0.18[0]	8.80±0.80[−1]	2.55±0.36[−1]	7.90±1.20[−2]	2.70±0.50[−2]	5.84±0.46[−3]
KP	4.12[1]	1.66[1]	5.68[0]	2.08[0]	8.21[−1]	2.60[−1]	8.09[−2]	2.35[−2]	5.59[−3]
1112									
Expt.	4.07±0.37[1]	1.62±0.16[1]	5.24±0.47[0]	1.85±0.18[0]	8.00±0.50[−1]	2.54±0.30[−1]	6.40±0.80[−2]	2.30±0.40[−2]	4.24±0.68[−3]
KP	3.90[1]	1.58[1]	5.30[0]	1.94[0]	7.74[−1]	2.37[−1]	7.45[−2]	2.18[−2]	4.99[−3]
1275									
Expt.	3.15±0.31[1]	1.08±0.12[1]	3.55±0.39[0]	1.27±0.17[0]	5.80±0.30[−1]	1.42±0.21[−1]		1.40±0.20[−2]	2.40±0.40[−3]
KP	2.82[1]	1.22[1]	3.40[0]	1.34[0]	5.57[−1]	1.28[−1]	4.77[−2]	1.43[−2]	2.42[−3]
1408									
Expt.	2.64±0.24[1]	9.50±0.90[0]	2.52±0.28[0]	1.01±0.10[0]	4.44±0.44[−1]	1.02±0.12[−1]	3.40±0.50[−2]	1.20±0.20[−2]	1.36±0.27[−3]
RMFF	2.22[1]	1.01[1]	2.43[0]	1.07[0]	4.21[−1]	8.94[−2]	4.06[−2]	1.25[−2]	1.82[−3]

isons of the experimental results with the $d\sigma^{KP}$ and $d\sigma^{RMFF}$ cross sections for Ta and U are shown in Figs. 1 and 2.

There are several sources of error which affect the determination of cross sections from Eq. (20). The error in the net elastic intensity arises from the combination of the uncertainty in determining the elastic intensity in the target spectrum and the uncertainty in determining the corresponding intensity in the background spectrum (no-target run). The error in an elastic intensity of a target spectrum for the case of well-separated elastic and Compton peaks ranged from 1% to 15% and arises from the counting statistics error and the uncertainty in determining the linear background underneath the peak. For the case of overlapping elastic and Compton peaks, the error in an elastic intensity ranged from 3% to 15% for γ rays of strong to weak intensity and was due to a combination of counting statistics error and the error from the least-squares method used for separating the elastic and Compton components. The least-squares method was the main source of error because of its sensitivity to channel shifts introduced to compensate for amplifier drifts for different runs. The total error in the net elastic intensity generally ranged from 2% to 20%.

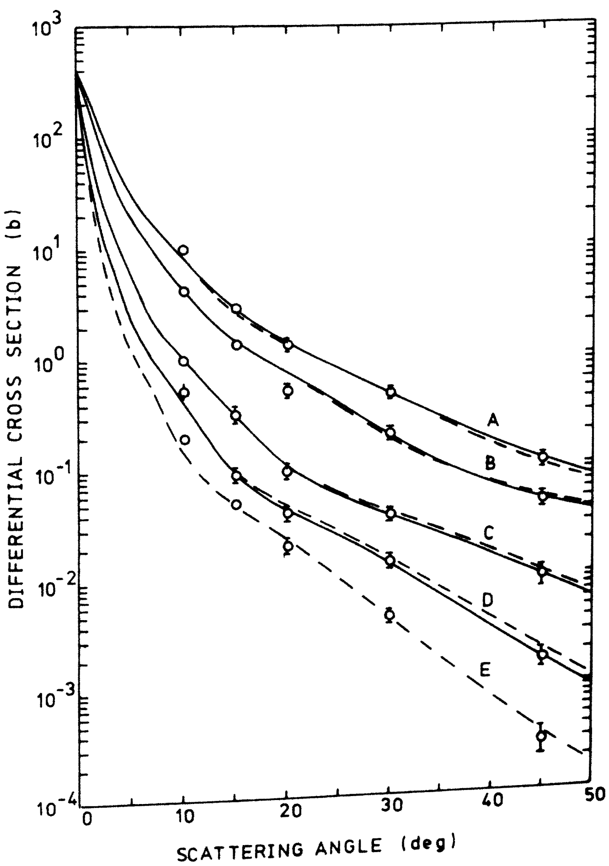

FIG. 1. Comparison of experimental differential elastic cross sections (denoted by ○) for Ta with theoretical Kissel-Pratt cross sections (Ref. 4) (solid line) and modified form-factor cross sections (dashed line) for scattering of 344-, 444-, 779-, 1086-, and 1408-keV γ rays, denoted by A, B, C, D, and E, respectively.

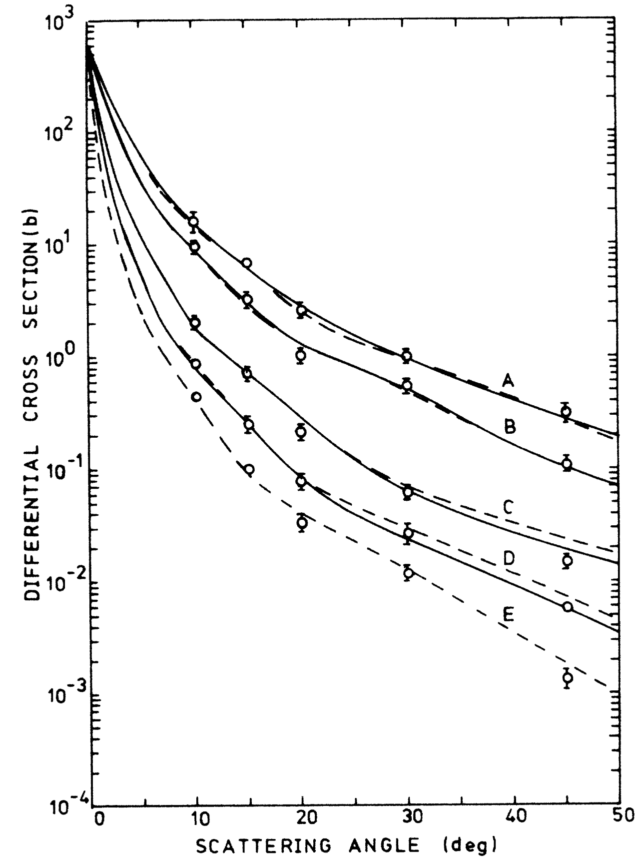

FIG. 2. As for Fig. 1 but for scattering by U.

Since the absolute source strength is not used for the determination of the elastic cross sections, self-absorption in the source had no effect on the measurements and therefore no correction was needed for this effect. The error in the value of the atomic density n_Z of a target used in the calculation was negligible since the mass density of a target could be easily determined to an accuracy of better than 0.5%. The error in the target transmission factor T depends on the product μt of the linear attenuation coefficient μ and the target thickness t. The values of μ were obtained from the tabulated mass-attenuation coefficients μ/ρ of Hubbell[28] and are accurate to better than a few percent. Apart from the uranium target, all target thicknesses satisfied $\mu t < 2$, resulting in a maximum error in T of 6%. For photon energies above 779 keV, where $\mu t < 1$, the error in T was less than 3%. For the uranium target with $\mu t > 2$, the error in T was about 10%. The relative photopeak efficiencies of the detector for the Compton and elastic peaks ranged from 1.009 to 1.014 with an error of less than 1%.

The geometrical factors required when different source-target-detector geometries were used were determined at a given scattering angle from the average of the ratio of the elastic intensities of each peak in the Pb target spectra for the two different geometries. The resulting errors were less than 5%.

The remaining source of error was associated with the determination of the scattering angle. The zero angle, and hence each scattering angle, was determined to $\pm 0.1°$ by finding the position of maximum count rate for a no-target run and then checking this setting by measuring the peak positions of the strong γ lines Compton scattered through 15° and comparing these energies with the Compton formula for $\hbar\omega^{\text{Compton}}$. This error of $\pm 0.1°$ corresponded to a maximum error in the elastic cross sections of 5% at small scattering angles (2°–5°), 3% at 7°, and was negligible at larger angles. Although no correction for angular acceptance was made to the cross sections (even at 2° the horizontal and vertical angular acceptances were only 0.46° and 0.05°, respectively, and the averaged theoretical cross section over the detector face corresponded to a scattering angle of 2.025°), the associated error in the cross section ($\leq 2\%$) was included in the experimental error.

The experimental results for each target material studied were determined with thin and thick targets. They were generally in agreement to better than 10% but for some weak lines they differed up to 20% on the account of poor counting statistics. The average values of the thin- and thick-target results, for those in agreement to better than 10%, were used for the final results. However, for the thin- and thick-target results which differed by more than 10%, the following criterion, based upon considerations of best counting statistics, was applied; for γ rays of energies less than 779 keV the results for the thin targets were used whereas for γ rays of energies greater than 779 keV the results for the thick targets were used.

IV. DISCUSSION AND CONCLUSIONS

The present experimentally measured elastic scattering cross sections are compared with theoretical elastic scattering cross sections, for Rayleigh plus nuclear-Thomson plus Delbruck scattering, in Tables I–VI and in Figs. 1 and 2. Only two theoretical models, $d\sigma^{\text{KP}}/d\Omega$ and $d\sigma^{\text{RMFF}}/d\Omega$, have been used for comparison since, as discussed earlier, the RMFF approximation is believed to be the most accurate model among the various form-factor approximations used for predicting the Rayleigh scattering amplitudes. The present experimental results are generally in excellent agreement to better than the 10% level with both theoretical models where the two models coincide and are in better agreement with the Kane *et al.* cross sections, for most cases, where the two models are different. For the case of the 1408-keV γ rays, where Kane *et al.* cross sections are not available, the experimental results for all targets at $\theta < 20°$ are generally in good agreement of order of 0–3 % with RMFF cross sections; for $\theta > 20°$ the experimental results for the lighter elements (Mo and Sn) are in reasonable agreement at the 15% level with the RMFF cross sections, but for heavier elements (Ta, Pb, and U) the experimental results apparently lie below the RMFF cross sections (by 2–15 %) as one would expect since the RMFF approximation has a tendency to over estimate the Rayleigh scattering amplitudes in such regions.

A direct comparison of the present experimental results with the results of other workers is difficult because of the rapid variation of the cross section with scattering angle and γ-ray energy. Therefore the comparison has been restricted to only those investigations which used equal or nearly equal γ-ray energies and/or scattering angles.

The only reported work using the same γ-ray energies and the same targets is that of Ramanathan *et al.*[29] This study only involved the measurement of elastic cross sections in the angular range from 2.4°–10°, and a comparison of their results with the present results has already been given.[1] In general, the present results for Cu are the same as that of Ramanathan *et al.*, but for the cases of Ta and especially Pb the present results lie above those of Ramanathan *et al.*

For those investigations which use the same targets and scattering angles but different energy γ rays to those of the present investigation, a direct comparison based upon the energy dependence of the present data is possible. Where only the target element is common with the present investigation, the results were interpolated to our scattering angles using the angular dependence of the theoretical cross sections of Kane *et al.* By restricting this interpolation to those experimental results of other workers where the change in cross section produced by the interpolation was less than 20%, the additional error in these results resulting from this interpolation should be less than 5%. From the experimental results so obtained,[30,31] the following conclusions can be drawn.

For the Cu target the present results are in good agreement at the 10% level with those of Kane *et al.*[32] and Sen Gupta *et al.*,[33] except the result of Kane *et al.* for 1333-keV γ rays at 5°, which is about 20% larger than the present result and is even larger than their own result for 1173-keV γ rays at 5°. However, it is only one case and the difference is still within the combined experimental error of both results. Our Cu results are also in reasonable agreement of the order of 5–20 % with those of de Barros *et al.*[34,35] and Goncalves *et al.*[36]

For Mo the present results agree to within 5–20 % with those of de Barros *et al.*[34,35] and to within 15% of those of Basavaraju *et al.*[37] For the case of the Sn target, the present results are in good agreement at the 10% or better level with those of Sen Gupta *et al.*,[33] Kane *et al.*,[32] and Goncalves *et al.*[36] but only in reasonable agreement of the order of 10–30 % with those of de Barros *et al.*[34,35] For the case of Ta, the other experimental results are limited; the result of Satyaendra Prasad *et al.*,[38] for the one overlapping case of 279-keV γ rays scattered through Ta at 45°, agrees to better than 5% with the present experimental result and the results of Smend *et al.*,[39] for 279- and 662-keV γ rays scattered by a Ta target at 45°, are in excellent agreement to better than 5% with the present experimental results. For the results of Basavaraju *et al.*[37] for Ta at 30°, their result for 1.17-MeV γ rays agrees within 10% with the general trend of the present results but their result for 1.33 MeV is 40% lower than the present result. This sizable difference may be due to the fact that the present result for 1.408-MeV γ rays lies above the general trend of the present results and their result for 1.33-MeV γ rays lies much lower than this trend (although their result for 1.17-MeV γ rays lies on this trend).

For the Pb target, the present results are in excellent agreement (see Fig. 3) at the 10% or better level with those of Schumacher,[40] Schumacher *et al.*,[41] Smend *et al.*,[39] Sen Gupta *et al.*,[33] Basavaraju *et al.*,[37] Kane *et al.*[32] and Goncalves *et al.*,[36] but are only in reasonable agreement with those of Dixon and Storey,[42] Hardie *et al.*,[43] Satyaendra Prasad *et al.*[38] and de Barros and coworkers;[34,35] the differences being 10–35 %, 5–30 %, 15%, and 5–20 %, respectively. There are significant differences between the present results and the early investigations of Wilson,[44] Mann,[45] Standing and Jovanovich,[46] and Narasimha Murty *et al.*[47] Finally for the case of the U target, the present results are, in most cases, in good agreement at the 10% level with those of Hardie *et al.*,[43] Muckenheim and Schumacher,[48] and Goncalves *et al.*,[36] the exceptions being γ-ray energies above 889 keV at 15°, where the present results lie 30% above those of Muckenheim and Schumacher. However, the differences are approximately the sizes of the combined experimental errors of both sets of results.

Recently Bradley and Ghose[49] have measured the scattering of 661.6-keV γ rays by Sn and Pb over scattering angles from 10.5°–60° and argued that there is a significant discrepancy between experiment and theory at 10.5°, with their results lying 50% below the calculations of Kane *et al.* Our results are in close agreement with their results for 20° and 30° scattering by Sn and Pb, and for 45° scattering by Pb, but disagree with their low 10.5° results. Goncalves *et al.*[36] have also recently measured the cross sections for 10.5° scattering of 661.6-keV γ rays by Sn and Pb and find no evidence for any discrepancy with the calculations of Kane *et al.*

The present investigation has reported on measurements of elastic scattering cross sections for scattering angles up to 45°. Even in this region many elastic cross sections could not be obtained because of very small elastic intensities. Although extension of the investigation to larger angles, where Delbruck scattering is even more significant, is clearly desirable, there are serious difficulties in using a multiline γ source such as Eu for such an investigation. At these larger angles the Compton peaks dominate the elastic peaks, and the Compton energy shifts increase, with the result that most of the elastic peaks will be small and overlaid by large Compton peaks. An investigation is currently underway to examine whether the increased intensities resulting from switching from transmission to reflection scattering will be sufficient to obtain some 60° and even 75° results, at least for the strong Eu γ lines and heavier targets. Extension of the measurements using the Eu source to very large angles does not seem possible.

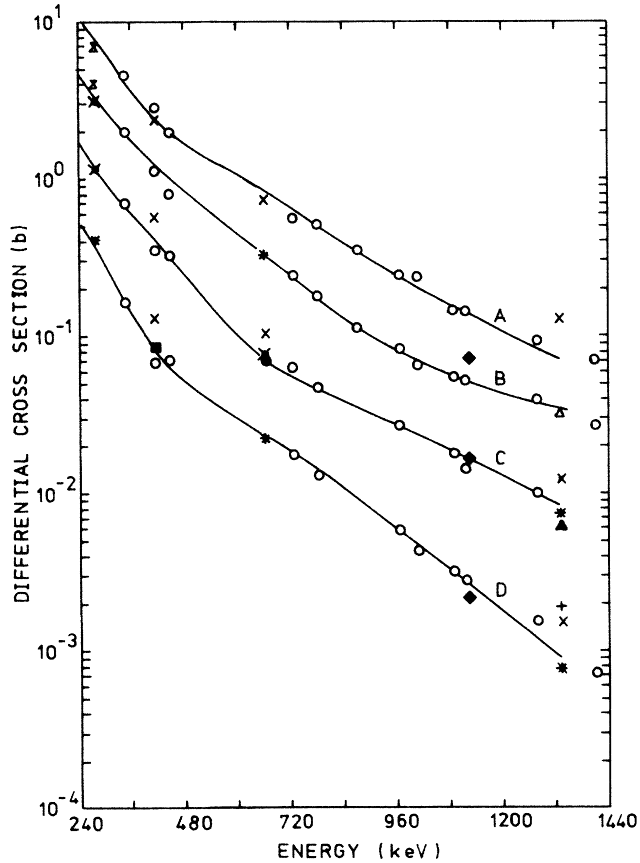

FIG. 3. Comparison of experimental differential elastic cross sections for Pb with theoretical Kissel-Pratt cross sections (solid line) for scattering through 15°, 20°, 30°, and 45°, denoted by *A*, *B*, *C*, and *D*, respectively. The experimental results shown are ○, present work; ✱, Bradley and Ghose (Ref. 49); ●, Goncalves *et al.* (Ref. 36); ■, Schumacher (Ref. 40); △, Hardie *et al.* (Ref. 43); ⧗, Nath and Ghose (Ref. 50); ♦, Narasimha Murty *et al.* (Ref. 47); ×, Mann (Ref. 45); +, Wilson (Ref. 44); and ▲, Dixon and Storey (Ref. 42). The symbol ∗ denotes the following composite sets of data: 30° scattering of 1330-keV γ rays (Refs. 43, 46, and 47); 45° scattering of 279-keV γ rays (Refs. 38, 39, and 40), 45° scattering of 662-keV γ rays (Refs. 36, 39, 40, and 45) and 45° scattering of 1330-keV γ rays (Refs. 42, 43, and 46).

ACKNOWLEDGMENTS

The authors would like to thank Professor R. H. Pratt and Dr. L. Kissel for providing tabulations of theoretical cross sections in advance of publication, and Professor K. Mork and Dr. T. Rotting for calculations of Delbruck scattering amplitudes. One of the authors (P.T.) would like to acknowledge financial assistance from the Australian Government under the Colombo Plan Scheme. This work was supported by a grant from the Australian Research Grants Scheme.

*Permanent address: Department of Applied Physics, King Mongkut Institute of Technology, Lad-Krabang Campus, Bangkok, Thailand 10520.

[1]R. B. Taylor, P. Teansomprasong, and I. B. Whittingham, Phys. Rev. A 32, 151 (1985).
[2]W. R. Johnson and F. D. Feiock, Phys. Rev. 168, 22 (1968); W. R. Johnson and K. Cheng, Phys. Rev. A 13, 692 (1976).
[3]L. Kissel, R. H. Pratt, and S. C. Roy, Phys. Rev. A 22, 1970

(1980); L. Kissel and R. H. Pratt, in *Atomic Inner-Shell Physics,* edited by B. Crasemann (Plenum, New York, 1985).
[4]P. P. Kane, L. Kissel, R. H. Pratt, and S. C. Roy, Phys. Rep. **140**, 75 (1986).
[5]W. Franz, Z. Phys. **98**, 314 (1935).
[6]L. Kissel and R. H. Pratt, Lawrence Livermore Laboratory Report No. XRM-78-107, 1978 (unpublished).
[7]P. Papatzacos and K. Mork, Phys. Rev. D **12**, 206 (1975).
[8]T. Bar-Noy and S. Kahane, Nucl. Phys. A **288**, 132 (1977).
[9]S. C. Roy, L. Kissel, and R. H. Pratt, Phys. Rev. A **27**, 285 (1983).
[10]R. B. Taylor, P. Teansomprasong, and I. B. Whittingham, Nucl. Instrum. Methods A **255**, 68 (1987).
[11]G. E. Brown, R. E. Peierls, and J. B. Woodward, Proc. R. Soc. London, Ser. A **227**, 51 (1954); S. Brenner, G. E. Brown, and J. B. Woodward, *ibid.* **227**, 59 (1954); G. E. Brown and D. F. Mayers, *ibid.* **234**, 387 (1956).
[12]J. S. Levinger, Phys. Rev. **87**, 656 (1952).
[13]G. E. Brown and D. F. Mayers, Proc. Phys. R. Soc. London, Ser. A **242**, 89 (1957).
[14]G. E. Brown and J. B. Woodward, Proc. Phys. Soc. London, Sec. A **65**, 977 (1952).
[15]J. S. Levinger and M. L. Rustgi, Phys. Rev. **103**, 439 (1956).
[16]V. Constantini, B. de Tollis, and G. Pistoni, Nuovo Cimento A **2**, 733 (1971); B. de Tollis, M. Lusignoli, and C. Pistoni, *ibid.* **32**, 227 (1976); B. de Tollis and G. Pistoni, *ibid.* **42**, 499 (1979).
[17]K. Mork and T. Rotting (private communication).
[18]P. Rullhusen, F. Smend, M. Schumacher, A. Hanser, and H. Rebel, Z. Phys. A **293**, 287 (1979).
[19]B. L. Berman and S. C. Fultz, Rev. Mod. Phys. **47**, 713 (1975).
[20]F. N. Fritsch and R. E. Carlson, Siam J. Numer. Anal. **17**, 238 (1980); F. N. Fritsch and J. Butland, Siam. J. Sci. Stat. Comput. **5**, 300 (1984).
[21]D. Schaupp, M. Schumacher, and F. Smend, Comput. Phys. Commun. **32**, 413 (1984).
[22]D. A. Liberman and D. T. Cromer, Comput. Phys. Commun. **2**, 107 (1971).
[23]D. Schaupp, M. Schumacher, F. Smend, P. Rullhusen, and J. H. Hubbell, J. Phys. Chem. Ref. Data **12**, 467 (1983).
[24]P. Teansomprasong and I. B. Whittingham, Natural Philosophical Research Report No. 79, James Cook University, 1985.
[25]W. Chitwattanagorn, R. B. Taylor, P. Teansomprasong, and I. B. Whittingham, J. Phys. G **6**, 1147 (1980).
[26]R. B. Taylor, P. Teansomprasong, and I. B. Whittingham, Aust. J. Phys. **34**, 125 (1981).
[27]J. C. Dow, G. C. Hicks, R. B. Taylor, and I. B. Whittingham, Nucl. Instrum. Methods A **255**, 78 (1987).
[28]J. H. Hubbell, Int. J. Appl. Radiat. Isot. **33**, 1269 (1982).
[29]N. Ramanathan, T. J. Kennett, and W. V. Prestwich, Can. J. Phys. **57**, 343 (1979).
[30]P. Teansomprasong, Ph.D. thesis, James Cook University, 1986.
[31]J. P. Lestone, Ph.D. thesis, James Cook University, 1986.
[32]P. P. Kane, J. Mahajani, G. Basavaraju, and A. K. Priyadarsini, Phys. Rev. A **28**, 1509 (1983).
[33]S. K. Sen Gupta, N. C. Paul, S. C. Roy, and N. Chaudhuri, J. Phys. B **12**, 1211 (1979).
[34]S. de Barros, J. Eichler, M. Gaspar, and O. Goncalves, Phys. Rev. C **24**, 1765 (1981).
[35]S. de Barros, J. Eichler, O. Goncalves, and M. Gaspar, Z. Naturforsch. **36a**, 595 (1981).
[36]O. Goncalves, S. de Barros, M. Gaspar, A. M. Goncalves, and J. Eichler, Z. Phys. D **1**, 167 (1986).
[37]G. Basavaraju, P. P. Kane, and K. M. Varier, Pramana **12**, 665 (1979).
[38]M. Satyaendra Prasad, G. Kusa Raju, K. Narasimha Murty, V. A. Narasimha Murty, and V. Lakshminarayana, Indian J. Pure Appl. Phys. **16**, 836 (1978).
[39]F. Smend, M. Schumacher, and I. Borchert, Nucl. Phys. A **213**, 309 (1973).
[40]M. Schumacher, Phys. Rev. **182**, 7 (1969).
[41]M. Schumacher, F. Smend, and I. Borchert, Nucl. Phys. A **206**, 531 (1973).
[42]W. R. Dixon and R. S. Storey, Can. J. Phys. **46**, 1153 (1968).
[43]G. Hardie, J. S. De Vries, and C. Chiang, Phys. Rev. C **3**, 1287 (1971).
[44]R. R. Wilson, Phys. Rev. **90**, 720 (1953).
[45]A. K. Mann, Phys. Rev. **101**, 4 (1956).
[46]K. G. Standing and J. V. Jovanovich, Nature **182**, 521 (1958).
[47]V. A. Narasimha Murty, V. Lakshminarayana, and J. Jnanananda, Nucl. Phys. **62**, 296 (1965).
[48]W. Muckenheim and M. Schumacher, J. Phys. G **6**, 1237 (1980).
[49]D. A. Bradley and A. M. Ghose, Phys. Rev. A **33**, 191 (1986).
[50]A. Nath and A. M. Ghose, Nucl. Phys. **57**, 547 (1964).